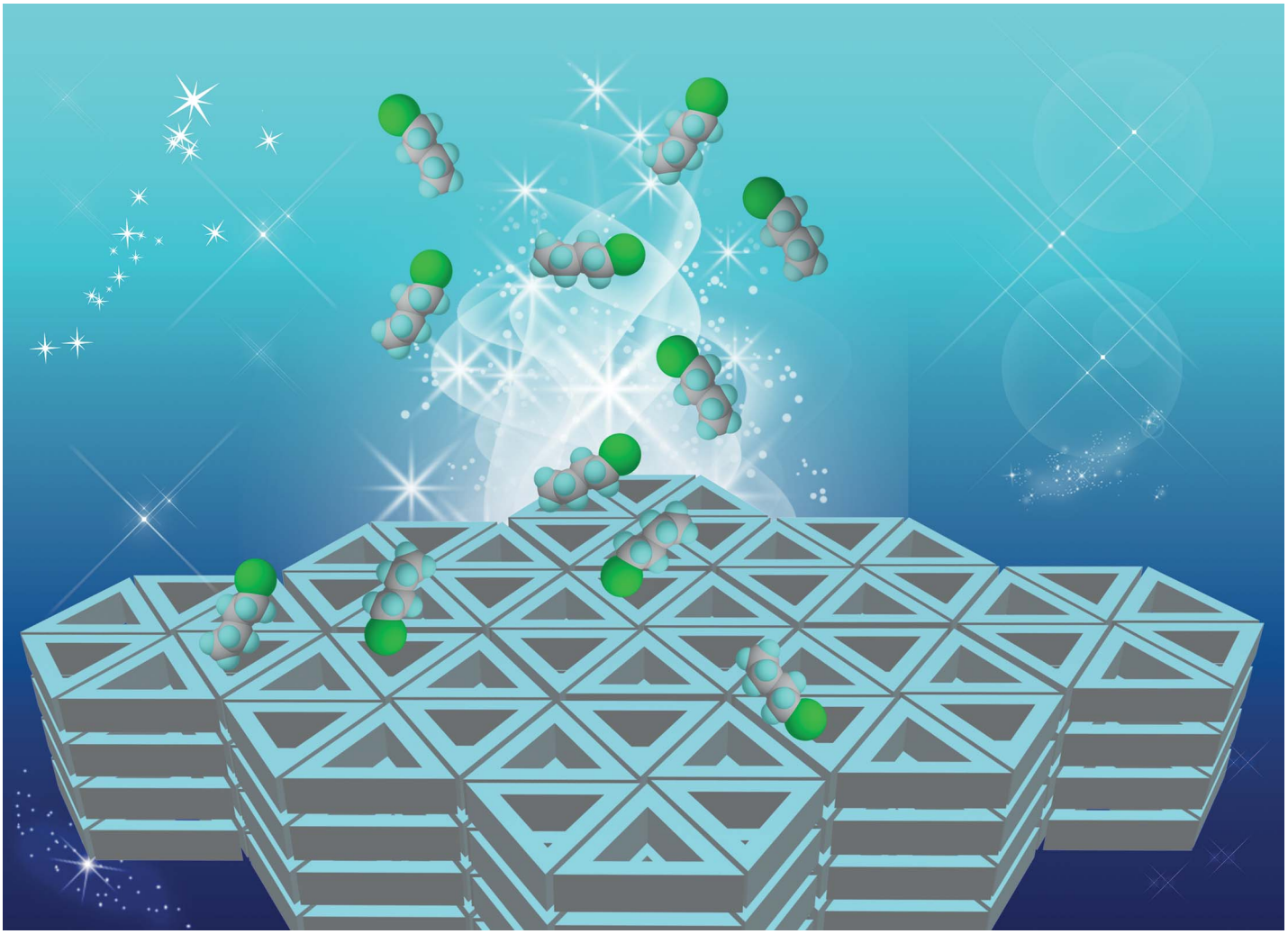

Showcasing research from Professor Khashab's laboratory, Chemical science program, King Abdullah University of Science and Technology, Thuwal, Kingdom of Saudi Arabia.

Tuning the porosity of triangular supramolecular adsorbents for superior haloalkane isomer separations

In this work, we investigated three different trianglamine/trianglimine macrocycles and tested their ability to successfully separate halobutane isomers. Methylene-bridged trianglamine (**TA**) was found to capture preferentially 1-chlorobutane (**1-CBU**) from a mixture of **1-CBU** and 2-chlorobutane (**2-CBU**) with a purity of 98.1%. Based on single crystal X-ray diffraction analyses, a thermodynamically stable [3]pseudorotaxane structure (**2TA⊃1-CBU**) is formed between **TA** and **1-CBU** that is characterized by an increased level of noncovalent interactions compared to the corresponding [2] pseudorotaxane structure seen for **TA⊃2-CBU**.

As featured in:

See Niveen M. Khashab *et al.*, *Chem. Sci.*, 2021, **12**, 12286.

ROYAL SOCIETY OF CHEMISTRY

rsc.li/chemical-science

Registered charity number: 207890

Chemical Science

ROYAL SOCIETY OF CHEMISTRY

EDGE ARTICLE

View Article Online
View Journal | View Issue

Cite this: *Chem. Sci.*, 2021, **12**, 12286

All publication charges for this article have been paid for by the Royal Society of Chemistry

Tuning the porosity of triangular supramolecular adsorbents for superior haloalkane isomer separations†

Bin Hua,[a] Yanjun Ding,[a] Lukman O. Alimi,[a] Basem Moosa,[a] Gengwu Zhang,[a] Walaa S. Baslyman,[a] Jonathan Sessler [b] and Niveen M. Khashab [*a]

Received 27th June 2021
Accepted 14th August 2021

DOI: 10.1039/d1sc03509f

rsc.li/chemical-science

Distillation-free separations of haloalkane isomers represents a persistent challenge for the chemical industry. Several classic molecular sorbents show high selectivity in the context of such separations; however, most suffer from limited tunability or poor stability. Herein, we report the results of a comparative study involving three trianglamine and trianglimine macrocycles as supramolecular adsorbents for the selective separation of halobutane isomers. Methylene-bridged trianglamine, **TA**, was found to capture preferentially 1-chlorobutane (**1-CBU**) from a mixture of **1-CBU** and 2-chlorobutane (**2-CBU**) with a purity of 98.1%. It also separates 1-bromobutane (**1-BBU**) from a mixture of **1-BBU** and 2-bromobutane (**2-BBU**) with a purity of 96.4%. The observed selectivity is ascribed to the thermodynamic stability of the **TA**-based host–guest complexes. Based on single crystal X-ray diffraction analyses, a [3] pseudorotaxane structure (**2TA⊃1-CBU**) is formed between **TA** and **1-CBU** that is characterized by an increased level of noncovalent interactions compared to the corresponding [2]pseudorotaxane structure seen for **TA⊃2-CBU**. We believe that molecular sorbents that rely on specific molecular recognition events, such as the triangular pores detailed here, will prove useful as next generation sorbents in energy-efficient separations.

Introduction

Haloalkanes are commercially important raw materials for the production of PVC, industrial lubricants, pesticides, insecticides, herbicides and many others.[1] They are generally produced through the direct halogenation of alkanes to produce a mixture of isomers, which are consequently separated by energy-intensive extractive and azeotropic distillations.[2–5] With an expected global market of 75.5 billion dollars by 2027, this segment of the chemical industry would benefit from economically advantageous access to 1-halo butanes such as 1-chlorobutane (**1-CBU**) and 1-bromobutane (**1-BBU**).[6,7] However, the efficient separation of these products from a mixture of isomers produced upon initial halogenation still constitutes a major obstacle towards their production under distillation-free, energy-efficient conditions.

High-performance molecular adsorbents for energy-saving isomer separations, including zeolites and metal–organic frameworks (MOFs), have been actively developed over the past few decades.[8,9] While precise control over the pore structure and hence separation selectivity has proved challenging in the case of classic zeolites, a lack of long term stability has emerged as the main factor limiting translation of many MOF-based platforms into the area of petrochemical separations.[10,11] On the other hand, considerable current effort is being focused on the development of new molecular and supramolecular adsorbents endowed with tunable structures and good stabilities; many show promise as next generation so-called smart separation materials.[12–17]

Molecular sorbents possessing triangular channels often display excellent performance as reflected in, *e.g.*, hexane isomer and olefin/paraffin separations.[18–20] Trianglamine and trianglimine macrocycles, in particular, have emerged as selective hosts for various benzene derivatives.[21,22] Receptors of this generalized class are readily prepared and easy to scale up, and possess cavities whose size can be tuned through design.[22–25] As detailed below, we have now investigated three different trianglamine/trianglimine macrocycles and tested their ability to separate halobutane isomers (Fig. 1). The methylene-bridged trianglamine (**TA**) was found to be a particularly good supramolecular adsorbent and one that allowed the facile separation of 1-chlorobutane (**1-CBU**), 1-bromobutane (**1-**

[a]*Smart Hybrid Materials Laboratory (SHMs), Advanced Membranes and Porous Materials Center, King Abdullah University of Science and Technology (KAUST), Thuwal 23955-6900, Saudi Arabia. E-mail: niveen.khashab@kaust.edu.sa*

[b]*Department of Chemistry, The University of Texas at Austin, Austin, TX 78712-1224, USA*

† Electronic supplementary information (ESI) available: X-ray crystallographic files (CIF), experimental details, NMR spectra and other materials (PDF). CCDC 2056799–2056802 and 2079899. For ESI and crystallographic data in CIF or other electronic format see DOI: 10.1039/d1sc03509f

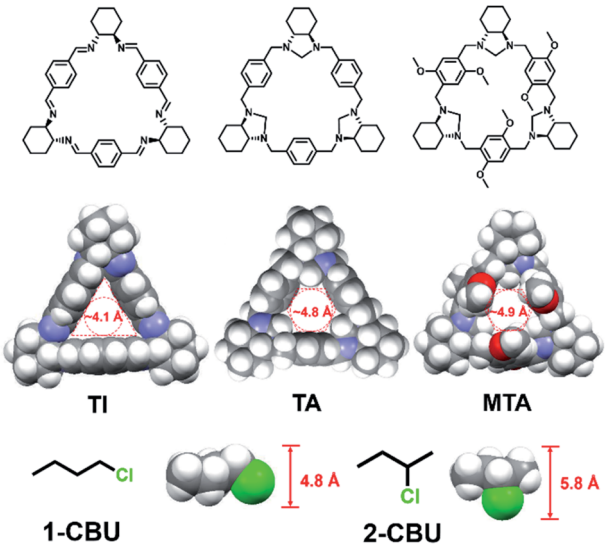

Fig. 1 Chemical structures of TI, TA, MTA, 1-chlorobutane (1-CBU) and 2-chlorobutane (2-CBU). The size of the cavities in TI, TA, and MTA were calculated to be 4.1, 4.8 and 4.9 Å, respectively. The effective sizes of 1-CBU and 2-CBU were calculated to be 4.8 and 5.8 Å, respectively.

BBU) and 1-chloropentane (**1-CP**) from mixtures of their corresponding isomers with purities of 98.1%, 96.4% and 97.1%, respectively. To the best of our knowledge, this is the first study that illustrates the importance of optimizing the pores of supramolecular adsorbents for various haloalkane separations and the origin of selectivity through the formation of pseudorotaxane assemblies.

Results and discussion

Three molecular triangle-shaped hosts with different cavity sizes were first selected as potential sorbents of chlorobutane isomers (Fig. 1). They were readily prepared *via* a simple condensation reaction as previously reported (Fig. S1–S4†).[26] Trianglimine (**TI**) has a rigid triangular cavity with a diameter of ~4.1 Å. The use of a different bridge between the aromatic subunits allowed access to a more hexagonal host, methylene-bridged trianglamine (**TA**), with an extended cavity whose effective size was increased to ~4.8 Å without the loss of structural rigidity. The corresponding dimethoxylated trianglamine (**MTA**), containing deeper cavities compared to **TA**, was also prepared (Fig. S5–S7†).

Guest-free **TI**, **TA** and **MTA** were converted to materials expected to be activated adsorptive separation materials *via* recrystallization and desolvation (Fig. S8–S10†).[27–30] These activated **TI**, **TA** and **MTA** crystalline materials were characterized by powder X-ray diffraction (PXRD) analyses that served to confirm their crystallinity (Fig. S11†).[31–34] Thermogravimetric analysis (TGA) of the activated **TI**, **TA** and **MTA** revealed no appreciable weight loss below 280 °C, thus providing support for the conclusion that these activated materials were fully desolvated (Fig. S12–S14†). N_2 adsorption experiments gave BET surface areas of 1.67 $m^2\ g^{-1}$, 3.65 $m^2\ g^{-1}$, and 1.74 $m^2\ g^{-1}$ for the activated **TI**, **TA** and **MTA**, respectively (Fig. S15–S17†). Although these values are low, previous reports on triangular macrocycles with little apparent porosity have served to reveal interesting molecular recognition features.[21,22,33]

The adsorption performance of the activated **TI**, **TA** and **MTA** in the presence of chlorobutane isomers was tested through

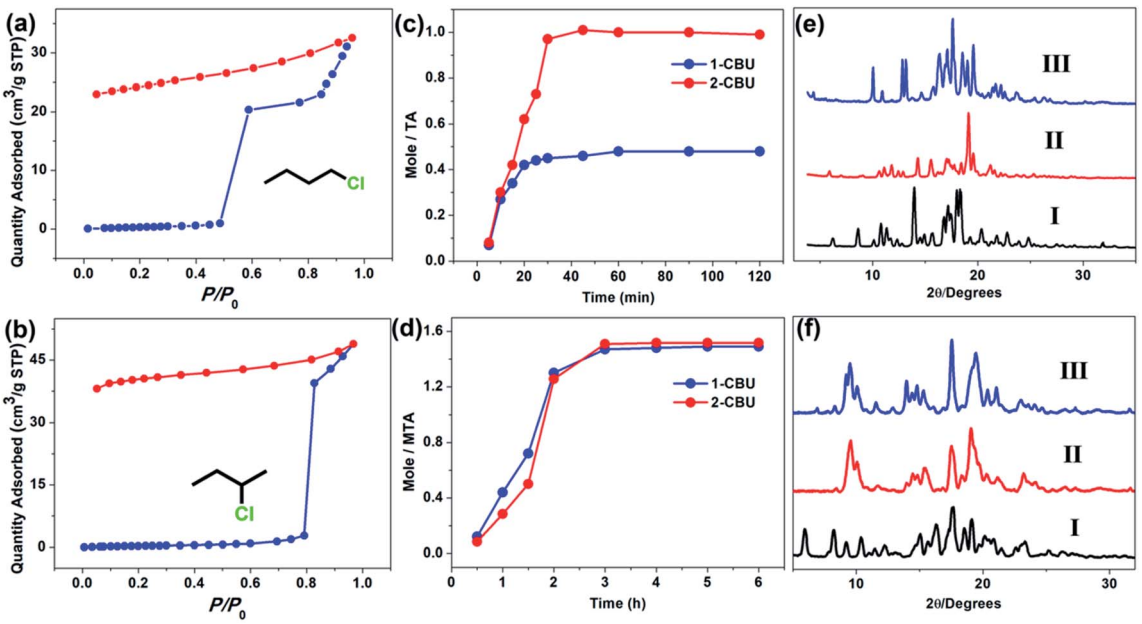

Fig. 2 Vapor sorption isotherms of (a) 1-CBU and (b) 2-CBU using activated TA as the putative absorbent at 298.15 K. Blue symbols: adsorption; red symbols: desorption. (c) Time-dependent solid–vapor sorption plot of activated TA for single-component chlorobutane isomer vapor. (d) Time-dependent solid–vapor sorption plot of activated MTA for single-component chlorobutane isomer vapor. (e) PXRD pattern of (I) activated TA; (II) activated TA after adsorption of 2-CBU vapor; (III) activated TA after adsorption of 1-CBU vapor. (f) PXRD pattern of (I) activated MTA; (II) activated MTA after adsorption of 2-CBU vapor; (III) activated MTA after adsorption of 1-CBU vapor.

solid–vapor adsorption experiments. Activated **TI** did not prove useful as an adsorbent for either **1-CBU** or **2-CBU** (Fig. S18†). In contrast, the vapor sorption isotherm for activated **TA** revealed that the adsorption of **1-CBU** and **2-CBU** was subject to pronounced gate-opening behavior at $P/P_0 = 0.5$ (for **1-CBU**) and $P/P_0 = 0.8$ (for **2-CBU**) (Fig. 2a and b). Analysis of the desorption process revealed that the adsorbed **1-CBU** and **2-CBU** molecules were not released, even under reduced pressure. This result was interpreted in terms of the chlorobutane isomers being stably located in the cavity of **TA** through host : guest interactions. We further investigated the binding using ^{1}H NMR spectroscopic analysis. On this basis, we conclude that **TA** accommodates **1-CBU** and **2-CBU** differently. In the case of **1-CBU**, two **TA** molecules bind a single **1-CBU** molecule while **2-CBU** binds **TA** with a 1 : 1 stoichiometry (Fig. S19 and S20†). The chlorobutane isomers were readily taken up by **TA** with *ca.* 30 minutes being required to reach the point of saturation (Fig. 2c). The larger receptor **MTA** adsorbs about 1.5 equiv. of **1-CBU** or **2-CBU** (Fig. S21 and S22†). Time-dependent solid–vapor studies with **MTA** and **1-CBU** and **2-CBU** revealed that close to 2 hours were required to reach saturation (Fig. 2d). We rationalize this relatively slow rate (compared to **TA**) in terms of the increased steric bulk of the methoxy groups of **MTA** serving to obstruct the entry of guests into the receptor cavity.

After confirming the adsorption of chlorobutane isomers by activated **TA** and **MTA**, the adsorption mechanism was further explored.[34] First PXRD was used to study the structural changes of the macrocycles before and after adsorption of **1-CBU** and **2-CBU**. As shown in Fig. 2e and f, the guest uptake induced a crystal to crystal transformation in these macrocycles. The PXRD pattern of activated **TA** drastically changed after adsorption of **2-CBU** and **1-CBU** (Fig. 2e, II and III). In contrast, in the case of activated **MTA**, almost no difference between the PXRD patterns of activated **MTA** after adsorption of **2-CBU** or **1-CBU** was seen (Fig. 2f, II and III), a finding interpreted in terms of the structures of this receptor remaining relatively unchanged upon the uptake of these two guests.

Single crystal X-ray diffraction (SCXRD) data confirmed that **TA** and **1-CBU** yielded a 2 : 1 host–guest complex and that the cavity of **TA** matched well with **1-CBU** (Fig. 3a). One **1-CBU** molecule was located in the cavity formed from two **TA** macrocycles to produce a threaded [3]pseudorotaxane structure **2TA⊃1-CBU**. Two C–H···π interactions and one C–H···Cl hydrogen bond were inferred from the metric parameters, which presumably contribute to the formation of the host–guest complex (Fig. S23†). The triangular macrocycles assemble in a 1D channel packing mode, with molecules **1-CBU** aligned within the channels. Notably, the PXRD spectrum of activated **TA** after the uptake of **1-CBU** was similar to the simulated pattern from the SCXRD data for **2TA⊃1-CBU** (Fig. S24†).

In contrast, **TA** and **2-CBU** were seen to form a 1 : 1 host–guest complex in the solid state on the basis of an SCXRD analysis. In this case a [2]pseudorotaxane structure **TA⊃2-CBU** was observed (Fig. 3b). Presumably reflecting the relatively

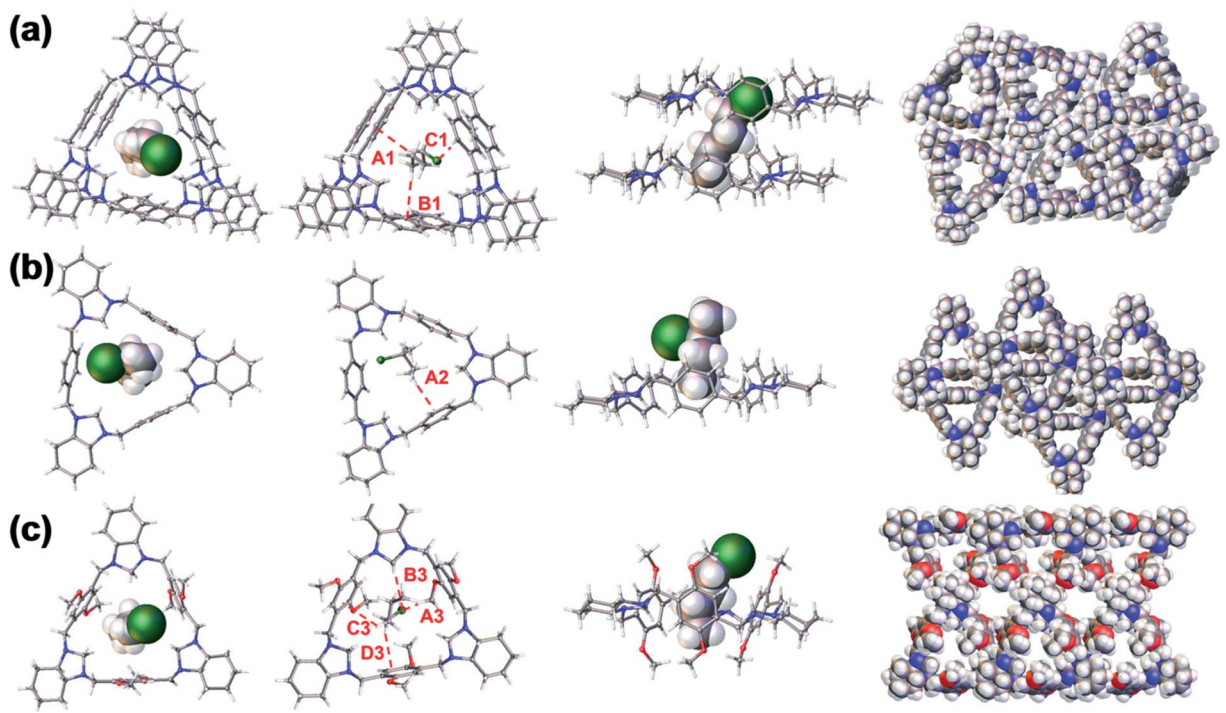

Fig. 3 Ball-stick views of the single crystal X-ray diffraction (SCXRD) structures of (a) **2TA⊃1-CBU**, (b) **TA⊃2-CBU** and (c) **MTA@1-CBU**. Red dashed lines show the noncovalent interactions existing between the host and the guest. In **2TA⊃1-CBU**, symbols A1 and B1 represent C–H···π interactions; symbol C1 represents C–H···Cl hydrogen bonds. In **TA⊃2-CBU**, symbol A2 represents C–H···π interactions. In **MTA@1-CBU**, symbols A3 and B3 represent C–H···Cl hydrogen bonds; symbols C3 and D3 represent C–H···π interactions (chlorobutanes were omitted for clarity).

larger size of **2-CBU** as compared to **1-CBU**, only the methyl group on **2-CBU** was seen to thread into the center of the cavity with binding driven by a single presumed C–H···π interaction (Fig. S25†). The complex **TA⊃2-CBU** does not produce a 1D channel-like structure, perhaps reflecting the fact that the adjacent **TA** macrocycles are staggered relative to one another. As in the case of **2TA⊃1-CBU**, the PXRD pattern of activated **TA** after adsorption of **2-CBU** (*i.e.*, **TA⊃2-CBU**) proved congruent with the simulated pattern derived from the single crystal data (Fig. S26†).

The SCXRD structure of **MTA@1-CBU** was also determined. It was found that the bound **1-CBU** molecules are located in the endo-cavity of **MTA** and in the extrinsic 1D channels (Fig. 3c and S27†). The molar ratio of **MTA** to **1-CBU** was calculated to be 1 : 1.5, which matched the results of solid–vapor adsorption experiments (Fig. S21†). The PXRD pattern of activated **MTA** after adsorption of **1-CBU** was the same as the simulated pattern from the single crystal structural data (Fig. S28†). The SCXRD analysis of **MTA@2-CBU** revealed a structure very similar to that of **MTA@1-CBU**. The **2-CBU** molecules were found in both the intrinsic and extrinsic 1D channels. Unfortunately, the SCXRD data could not be refined due to the disorder seen for the **2-CBU** molecules bound in the extrinsic channels (Fig. S29 and S30†). Nevertheless, these data and the corresponding PXRD analyses confirmed that crystallinity is retained as activated **MTA** adsorbs **2-CBU** vapor (Fig. S31†).

We next probed whether the crystalline forms of activated **TA** and **MTA** displayed selectivity towards a specific chlorobutane isomer. It was found that **TA⊃2-CBU** is transformed into **2TA⊃1-CBU** upon exposure to **1-CBU** vapor (Fig. 4a). At the saturation point, the content of **2-CBU** in the solid was almost negligible (Fig. 4a). Time-dependent PXRD analyses proved to be consistent with the crystal-to-crystal transformation of **TA⊃2-CBU** into **2TA⊃1-CBU** (Fig. 4b) and that the process was essentially irreversible (Fig. S32† and 4c). On this basis, we conclude that **2TA⊃1-CBU** is thermodynamically more stable than **TA⊃2-CBU**. We believe that the relatively high number of noncovalent interactions in the [3]pseudorotaxane structure of **2TA⊃1-CBU** serves to drive the equilibrium towards this dominant species.

Inspired by these initial experiments, we investigated the possibility of employing activated **TA** and activated **MTA** to separate **1-CBU** from an isomeric mixture of **1-CBU** and **2-CBU** (v/v = 1 : 1). Based on NMR spectroscopic analyses associated with the solid–vapor adsorption experiments, it was found that activated **MTA** failed to display selectivity toward either chlorobutane isomer (Fig. S33 and S34†). Gas chromatography (GC) studies revealed that after exposure to a 1 : 1 isomeric mixture of chlorobutane, the ratio of **1-CBU** to **2-CBU** in **MTA** was 51.5 : 48.5, (Fig. S35†). In marked contrast, **TA** can clearly discriminate **1-CBU** from **2-CBU** with high selectivity (Fig. S36†).

We further performed time-dependent solid–vapor adsorption studies of activated **TA** and an isomeric mixture consisting of **1-CBU** and **2-CBU**. These studies revealed that the uptake of **1-CBU** was essentially complete within 30 min while the amount of **2-CBU** absorbed over this time proved negligible (Fig. 5a). GC analysis revealed that the percentage of **1-CBU** in **TA** was 98.1% (Fig. 5b and S37†). Time-dependent PXRD studies revealed that

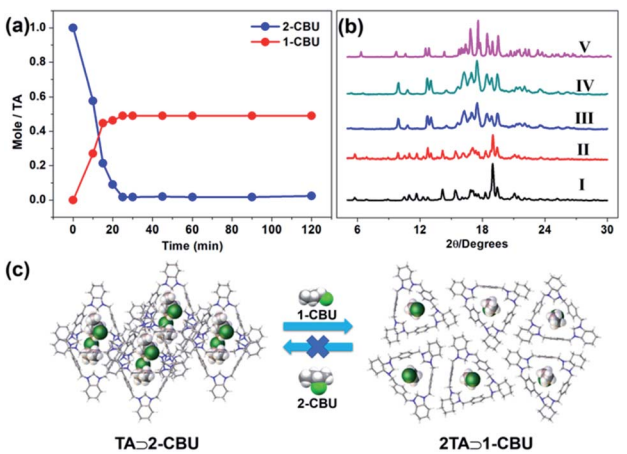

Fig. 4 (a) Time-dependent solid–vapor sorption plot of **TA⊃2-CBU** after exposure to **1-CBU** vapor. (b) Time-dependent PXRD pattern of (I) initial **TA⊃2-CBU**; **TA⊃2-CBU** after adsorption of **1-CBU** vapor for (II) 10 minutes; (III) 20 minutes and (IV) 30 minutes; (V) simulated pattern produced from the single crystal structural data for **2TA⊃1-CBU**. (c) Illustration showing the reversible and irreversible structural transformation between **TA⊃2-CBU** and **2TA⊃1-CBU**.

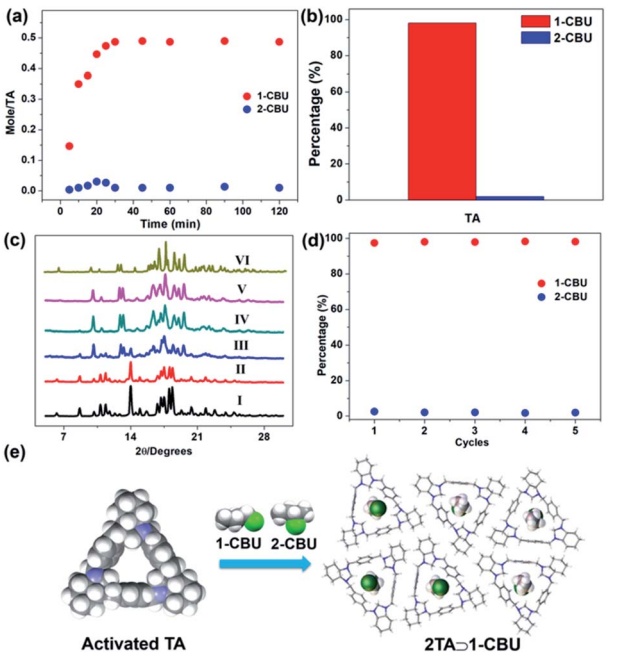

Fig. 5 (a) Time-dependent solid–vapor sorption plot of activated **TA** exposed to a 1 : 1 vapor mixture of **1-CBU** and **2-CBU**. (b) Percentages of **1-CBU** and **2-CBU** adsorbed by activated **TA**, as determined by GC analysis. (c) Time-dependent PXRD patterns of (I) activated **TA**, and activated **TA** after contact with a 1 : 1 mixture of **1-CBU** and **2-CBU** vapor for (II) 5 minutes, (III) 15 minutes, (IV) 30 minutes, and (V) 45 minutes. (VI) the simulated spectrum derived from the single crystal structural data for **2TA⊃1-CBU**. (d) Relative uptake of **1-CBU** and **2-CBU** through five cycles. (e) Schematic representation of the structural transformation from activated **TA** to **2TA⊃1-CBU** that is proposed to occur upon exposure to a 1 : 1 mixture of **1-CBU** and **2-CBU** vapor.

after exposure to a 1 : 1 mixture of **1-CBU** and **2-CBU**, the final PXRD pattern was similar to that of **2TA⊃1-CBU** (Fig. 5c). More importantly, activated **TA** could be recycled at least five times without losing its adsorption capacity and selectivity (Fig. 5d); it also proved to be stable in aqueous media (Fig. S38†).

We then tested the selectivity of activated **TA** towards other halobutanes such as bromobutanes (**BBU**). Notably, activated **TA** can discriminate 1-bromobutane (**1-BBU**) from 2-bromobutane (**2-BBU**) as confirmed by ^{1}H NMR and PXRD data (Fig. S39–S41†). GC results showed that the activated **TA** can selectively capture **1-BBU** from a mixture of **1-BBU** and **2-BBU** with a purity of 96.4%; excellent reusability was seen again (Fig. S42 and S43†). We also investigated the ability of **TA** to host other haloalkanes such as 1-chloropentane (**1-CP**). SCXRD data showed that when exposed to **1-CP**, **TA** forms 1D channels reminiscent of **2TA⊃1-CBU** (Fig. S44†). Moreover, we further found that activated **TA** can also be used to separate 1-chloropentane from a mixture of 1-chloropentane and 2-chloropentane with a purity of 97.1% (Fig. S45–S47†).

Conclusion

In conclusion, we investigated the adsorption performance of three trianglamine/trianglimine macrocycles **TI**, **TA**, and **MTA** upon exposure to chlorobutane isomers (**CBU**). It was found that **TI**, the system with the smallest cavity size within the series, was ineffective as an absorbent for either chlorobutane isomer (*i.e.*, **1-CBU** and **2-CBU**). In contrast, both **TA** and **MTA**, possessing relatively larger cavity sizes, proved to be effective adsorbents for both **1-CBU** and **2-CBU**. In both cases, saturation was reached in about 30 min, which is fast compared to literature reports of other molecular sorbents that can require up to 5 h to reach saturation.[7] Of particular note is the finding that **TA** could be used to separate **1-CBU** from a mixture of **1-CBU** and **2-CBU** with a purity of 98.1%. The selectivity is rationalized on thermodynamic grounds. Based on SCXRD analyses, a [3] pseudorotaxane structure, **2TA⊃1-CBU**, is formed in the case of **1-CBU** that is characterized by a greater number of noncovalent host : guest interactions compared to the [2]pseudorotaxane structure seen in the case of **TA⊃2-CBU**. Further studies revealed that **TA** can also separate 1-bromobutane (**1-BBU**) and 1-chloropentane from mixtures of their corresponding isomers with purities of 96.4% and 97.1%, respectively. Both **TA** and **MTA** proved to be stable under conditions of use and could be recycled and reused. The fact that these systems display excellent selectivity, and are easy to prepare and subject to preparative scale up leads us to predict that sorbents with triangular channels may see use in practical applications, particularly in energy-efficient small molecule separations.

Author contributions

N. M. K. concieved the concept and supervised the project. H. B. developed the concept and performed the majority of the experiments. All authors contributed to the analysis and writing.

Conflicts of interest

There are no conflicts to declare.

Acknowledgements

This work was supported by the Office of Sponsored Research (CRG4) at the King Abdullah University of Science and Technology (KAUST), Saudi Arabia.

References

1 M. Rossberg, W. Lendle, G. Pfleiderer, A. Togel, E.-L. Dreher, E. Langer, H. Rassaerts, P. Kleinschmidt, H. Strack, R. Cook, U. Beck, K.-A. Lipper, T. R. Torkelson, E. Loser, K. K. Beutel and T. Mann, *Chlorinated Hydrocarbons in Ullmann's Encyclopedia of Industrial Chemistry*, Wiley-VCH, Weinheim, 2000.
2 J. E. Copenhaver and A. M. Whaley, *Org. Synth.*, 1925, **5**, 27.
3 L. Vasaros, H. J. Machulla and W. Tornau, *J. Chromatogr. A*, 1971, **62**, 458–461.
4 L. H. Brandsma and D. Verkruijsse, *Preparative Polar Organometellic Chemistry I*, Springer-Verlag, Berlin, 1987, ISBN 3-540-16916-4.
5 P. Comba and S. Wunderlich, *Chem.–Eur. J.*, 2010, **16**, 7293–7299.
6 J.-R. Wu, B. Li and Y.-W. Yang, *Angew. Chem., Int. Ed.*, 2020, **59**, 2251–2255.
7 Y. Zhou, K. Jie, R. Zhao, E. Li and F. Huang, *J. Am. Chem. Soc.*, 2020, **142**, 6957–6961.
8 H. Li, M. Eddaoudi, M. O'Keeffe and O. Yaghi, *Nature*, 1999, **402**, 276.
9 A. Cadiau, K. Adil, P. M. Bhatt, Y. Belmabkhout and M. Eddaoudi, *Science*, 2016, **353**, 137–140.
10 S. M. Kuznicki, V. A. Bell, S. Mair, H. W. Hillhouse, R. M. Jacubinas, C. M. Braunbarth, B. H. Toby and M. Tsapatsis, *Nature*, 2001, **412**, 720–724.
11 R. E. Morris and L. Brammer, *Chem. Soc. Rev.*, 2017, **46**, 5444–5462.
12 M. A. Little and A. I. Cooper, *Adv. Funct. Mater.*, 2020, **30**, 1909842.
13 G. Zhang, A. H. Emwas, U. F. S. Hameed, S. T. Arold, P. Yang, A. Chen, J. F. Xiang and N. M. Khashab, *Chem*, 2020, **6**, 1082–1096.
14 W. Yang, K. Samanta, X. Wan, T. U. Thikekar, Y. Chao, S. Li, K. Du, J. Xu, Y. Gao, H. Zuilhof and A. C.-H. Sue, *Angew. Chem., Int. Ed.*, 2019, **59**, 3994–3999.
15 L. Chen, Y. Cai, W. Feng and L. Yuan, *Chem. Commun.*, 2019, **55**, 7883–7898.
16 G. Zhu, F. Zhang, M. P. Rivera, X. Hu, G. Zhang, C. W. Jones and R. P. Lively, *Angew. Chem., Int. Ed.*, 2019, **58**, 2638–2643.
17 S. Xie, S. Wu, S. Bao, Y. Wang, Y. Zheng, D. Deng, L. Huang, L. Zhang, M. Lee and Z. Huang, *Adv. Mater.*, 2018, **30**, 1800683.
18 Z. R. Herm, B. M. Wiers, J. A. Mason, J. M. v. Baten, M. R. Hudson, P. Zajdel, C. M. Brown, N. Masciocchi, R. Krishna and J. R. Long, *Science*, 2013, **340**, 960–964.

19 Z. Bao, J. Wang, Z. Zhang, H. Xing, Q. Yang, Y. Yang, H. Wu, R. Krishna, W. Zhou, B. Chen and Q. Ren, *Angew. Chem., Int. Ed.*, 2018, **57**, 16020–16025.
20 P. Wang, X. Chen, Q. Jiang, M. Addicoat, N. Huang, S. Dalapati, T. Heine, F. Huo and D. Jiang, *Angew. Chem., Int. Ed.*, 2019, **58**, 15922–15927.
21 A. Dey, S. Chand, L. O. Alimi, M. Ghosh, L. Cavallo and N. M. Khashab, *J. Am. Chem. Soc.*, 2020, **142**, 15823–15829.
22 A. Dey, S. Chand, B. Maity, P. M. Bhatt, M. Ghosh, L. Cavallo, M. Eddaoudi and N. M. Khashab, *J. Am. Chem. Soc.*, 2021, **143**, 4090–4094.
23 J. Gawronski, H. Kolbon, M. Kwit and A. Katrusiak, *J. Org. Chem.*, 2000, **65**, 5768–5773.
24 A. Chaix, G. Mouchaham, A. Shkurenko, P. Hoang, B. Moosa, P. M. Bhatt, K. Adil, K. N. Salama, M. Eddaoudi and N. M. Khashab, *J. Am. Chem. Soc.*, 2018, **140**, 14571–14575.
25 Y. Ding, L. O. Alimi, B. Moosa, C. Maaliki, J. Jacquemin, F. Huang and N. M. Khashab, *Chem. Sci.*, 2021, **12**, 5315–5318.
26 J. Gawronski, K. Gawronska, J. Grajewski, M. Kwit, A. Plutecka and U. Rychlewska, *Chem.–Eur. J.*, 2006, **12**, 1807–1817.
27 R. S. Patil, D. Banerjee, C. Zhang, P. K. Thallapally and J. L. Atwood, *Angew. Chem., Int. Ed.*, 2016, **55**, 4523–4526.
28 T. Ogoshi, K. Saito, R. Sueto, R. Kojima, Y. Hamada, S. Akine, A. M. P. Moeljadi, H. Hirao, T. Kakuta and T.-a. Yamagishi, *Angew. Chem., Int. Ed.*, 2018, **57**, 1592–1595.
29 J.-R. Wu and Y.-W. Yang, *Angew. Chem., Int. Ed.*, 2021, **60**, 1690–1701.
30 L. J. Barbour, *Chem. Commun.*, 2006, **11**, 1163–1168.
31 L. R. MacGillivray and J. L. Atwood, *Chem. Commun.*, 1999, **2**, 181–182.
32 K. Jie, Y. Zhou, E. Li and F. Huang, *Acc. Chem. Res.*, 2018, **51**, 2064–2072.
33 G. Zhang, B. Hua, A. Dey, M. Ghosh, B. A. Moosa and N. M. Khashab, *Acc. Chem. Res.*, 2021, **54**, 155–168.
34 B. Moosa, L. O. Alimi, A. Shkurenko, A. Fakim, P. M. Bhatt, G. Zhang, M. Eddaoudi and N. M. Khashab, *Angew. Chem., Int. Ed.*, 2020, **59**, 21367–21371.